Monatshefte für Chemie 138, 301–307 (2007)
DOI 10.1007/s00706-007-0614-5
Printed in The Netherlands

**Monatshefte für Chemie
Chemical Monthly**

# The Effect of Styrene-Butadiene-Styrene Modification on the Characteristics and Performance of Bitumen

**Klaus Stangl**[1,*], **Andreas Jäger**[2], and **Roman Lackner**[2,3]

[1] Christian Doppler Laboratory for "Performance-based Optimization of Flexible Pavements", Institute for Road Construction and Maintenance, Vienna University of Technology, Vienna, Austria
[2] Christian Doppler Laboratory for "Performance-based Optimization of Flexible Pavements", Institute for Mechanics of Materials and Structures, Vienna University of Technology, Vienna, Austria
[3] FG Computational Mechanics, Technical University of Munich, Munich, Germany

Received November 30, 2006; accepted (revised) January 30, 2007; published online March 29, 2007


**Summary.** In order to cover the effect of styrene-butadiene-styrene (*SBS*) modification on the characteristics of bitumen, two types of bitumen, one plain bitumen, and one polymer modified bitumen produced with the plain bitumen as base material were characterized in terms of chemical composition, microstructure, micromechanical properties, and thermoanalytical behavior. In order to determine the complex chemical composition of bitumen, elemental analysis, gel permeation chromatography, and the Iatroscan method were employed. Microstructure and micromechanical properties were determined using an environmental scanning electron microscope and the nanoindentation technique. Modulated differential scanning calorimetry was used to determine phase-change temperatures and endo/exotherms associated with molecular movement. The addition of *SBS* leads to different rheological behavior over the whole service temperature range. This is reflected in bitumen chemistry by differences in elemental composition and molecular weight distribution with much higher $M_w$ values for the modified bitumen. Accordingly, the polymer leads to a shift in molecular fractions. Electron microscopy reveals two distinct phases building up the bitumen microstructure. The chosen mode of quantification leads to similar material parameters for both bitumens, which is explained by the use of the same base material. In contrast, nanoindentation delivers viscosities in the micro-range corresponding to large-scale rheological properties. Modulated differential scanning calorimetry indicates two glass transitions corresponding with two material phases also confirmed by other experiments. Due to modification, these glass transitions depart from each other and the amount of the two material phases changes, correlating with the shift in molecular fractions observed in Iatroscan analyses.

**Keywords.** Polymer-modified; Microstructure; Physico-chemical analyses.

## Introduction

Bitumen is the binder material of asphalt and the only material phase in asphalt exhibiting thermorheological properties. Consequently, the performance of asphalt in the different temperature regimes strongly depends on the used type of bitumen, its chemical composition, and microstructure. Bitumen is the remaining part of the crude-oil distillation. Hence, its chemical composition and its mechanical properties strongly depend on the origin of the crude oil and on the distillation process. Bitumen mainly consists of hydrocarbons together with sulfur, nitrogen, and oxygen. In addition, it contains metals in small quantities. This elemental composition results in the formation of a wide range of molecules, which are typically divided into four molecular groups [1]: saturates, aromatics, resins, and asphaltenes. Hereby, the molecular mass increases from the saturates (molecular weight from 300 to 2000 g/mol) to the asphaltenes (molecular weight from 1000 to 10000 g/mol). Moreover, the aromaticity and heteroatom content increase from the saturates to the

* Corresponding author. E-mail: kstangl@istu.tuwien.ac.at

asphaltenes in the same order. Due to these characteristics in the molecular composition, bitumen is referred to as a 'Molecular Cocktail'.

In order to optimize the aforementioned thermo-rheological properties of bitumen, polymers like thermoplastics or elastomers are added. Such a bitumen/polymer blend is referred to as 'polymer modified bitumen' (PmB). The polymer content of a PmB used in road construction ranges between 2.5 and 5% by weight. Both phases build a physical network but do not chemically react with each other yielding the bitumen as the continuous phase and the polymer phase being dispersed through it. Today, the most used polymer for bitumen modification is styrene-butadiene-styrene (*SBS*) block copolymer rich in butadiene (60–70%) followed by reclaimed tire rubber. *SBS* is incorporated into bitumen by the addition of solid polymers in a separate process and requires mixing and shearing in order to uniformly disperse the polymers. In addition to the properties of the original bitumen, the properties of modified bitumen depend on the characteristics of the polymer, the mixing conditions, and the compatibility of the polymer with the bitumen. The motivation to modify bitumen with polymers is twofold: first the viscosity of bitumen/polymer blends is lower at low service temperatures reducing the risk of low-temperature cracking. Second, blends show a higher viscosity at elevated temperatures leading to a reduced formation of permanent deformation ("rutting"). This positive effect of polymers on the rheological properties of bitumen is illustrated in Figs. 1 and 2 showing the results of dynamic shear rheometer (DSR) experiments (complex shear modulus $G^*$ and phase angle $\delta$) for the original and the modified bitumen. Hereby, $G^*$ is obtained as following:

$$G^* = \sqrt{(G')^2 + (G'')^2}, \tag{1}$$

where $G'$ denotes the storage modulus (elastic part) and $G''$ denotes the loss modulus (viscous part).

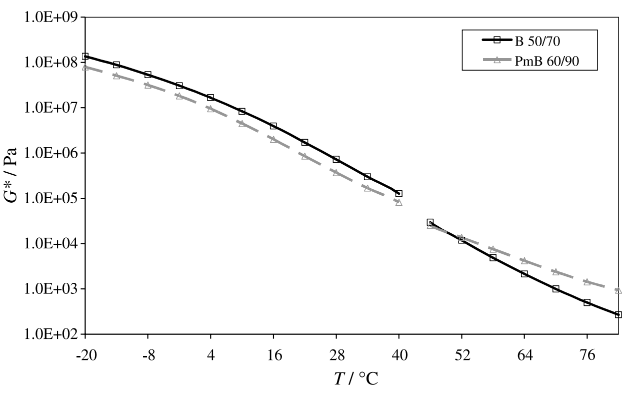


**Fig. 1.** Complex shear modulus $G^*$ (see definition in the text) for plain (B 50/70) and modified (PmB 60/90) bitumen

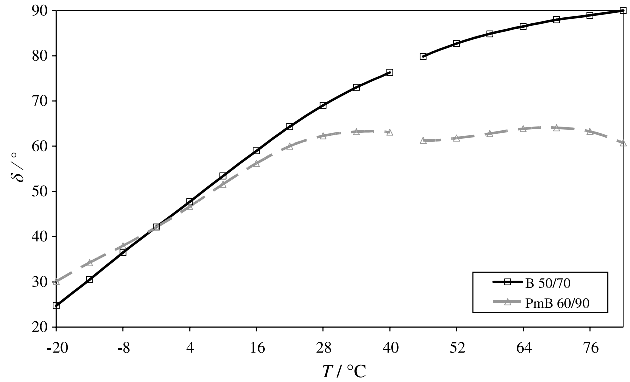


**Fig. 2.** Phase angle $\delta$ for plain (B 50/70) and modified (PmB 60/90) bitumen

The modified bitumen (denoted PmB 60/90) exhibits higher values for $G^*$ at elevated temperatures and lower values for $G^*$ at low temperatures. This behavior is also reflected by the phase angle $\delta$ with lower values for the modified bitumen for a broad temperature range indicating a more elastic material behavior in the medium and high temperature regime. According to these observations, the addition of polymers extends the temperature range of application [2, 3].

The origin of the observed improvement of rheological/mechanical properties of bitumen by polymer modification shall be explained in this paper, investigating the effect of polymer modification on the chemical composition, microstructure, and thermoanalytical behavior.

## Results and Discussion

### *Effect of Polymer Modification on Chemical Composition of Bitumen*

Elemental analysis (EA) reveals that the molecules are predominantly composed of carbon and hydrogen, with mass fractions of approximately 84 and 10% (see Table 1). Though B 50/70 was used as base material for the production of PmB 60/90, differences in the elemental composition between both binders are found as a result of the modification process. Whereas the oxygen content of B 50/70 is

**Table 1.** Elemental composition of considered types of bitumen

| Bitumen | $C$ [m%] | $H$ [m%] | $O$ [m%] | $N$ [m%] | $S$ [m%] |
|---|---|---|---|---|---|
| B 50/70 | 83.9 | 10.4 | <0.1 | 0.4 | 5.0 |
| PmB 60/90 | 84.3 | 10.3 | 0.6 | 0.4 | 4.3 |

negligible, PmB 60/90 shows an oxygen content of 0.6%. This increase of oxygen in consequence of the allowance of *SBS* is explained by oxygen attaching to the double bonds of *SBS*, with the latter being susceptible for oxidation. The sulfur content of B 50/70 is 5% and decreased by the allowance of *SBS* to 4.3%. This decrease results from the formation and, subsequently, evaporation of low molecular weight sulfur-containing components, such as hydrogen sulfide, during the modification process. Moreover, the soaking oil added for the modification process mainly contains hydrocarbons, also causing a decrease of the amount of oxygen, nitrogen, and sulfur.

The molecular weight distribution for the considered types of bitumen, obtained from gel permeation chromatography (GPC), is illustrated in Fig. 3. Since

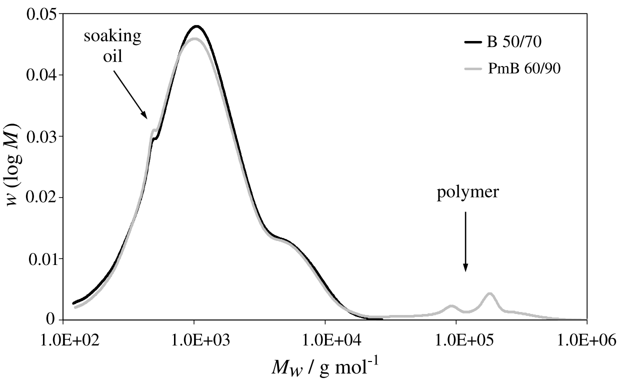


**Fig. 3.** Logarithmic differential mass distribution of molar mass, $M$, of B 50/70 and PmB 60/90

**Table 2.** Results from gel permeation chromatography: weight average molecular weight $M_w$

| Bitumen | $M_w$/g mol$^{-1}$ |
|---|---|
| B 50/70 | 1921 |
| PmB 60/90 | 8674 |

the molecular weight distributions shown in Fig. 3 are scaled with the respective area under each distribution summing up to 100%, the allowance of polymers results in a reduction of the maximum value of the GPC graph obtained for PmB 60/90. The increase of a little peak at around 500 g/mol may be explained by the soaking oil used in the production process of the PmB. In contrast to B 50/70, PmB 60/90 shows a small amount of large-weight molecules (with $M_w > 50000$ g/mol), corresponding to the styrene-butadiene-styrene content (with a mean value of around 250000 g/mol [4]). Hence, the weight average molecular weight $M_w$ (see Eq. (2) in subsequent section) representing both the original bitumen and *SBS* increases in consequence of polymer modification (Table 2).

In Fig. 4 typical chromatograms from Iatroscan experiments for both types of bitumen are presented and the mean values for the amount of generic fractions are summarized in Table 3 as percentage by area. In general, the conversion of area into weight percentage requires the use of correlation coefficients taking the different crude oil dependent C/H-ratios within every fraction into account. However, since the considered B 50/70 was used as base material in the production of the PmB 60/90, the observed results may be compared in a relative manner. While saturates ($S$) and asphaltenes ($As$) remain almost constant due to modification, aromatics ($A$) and resins ($R$) show high chemical reactivity. The addition of *SBS* leads to a shift from aromatics to

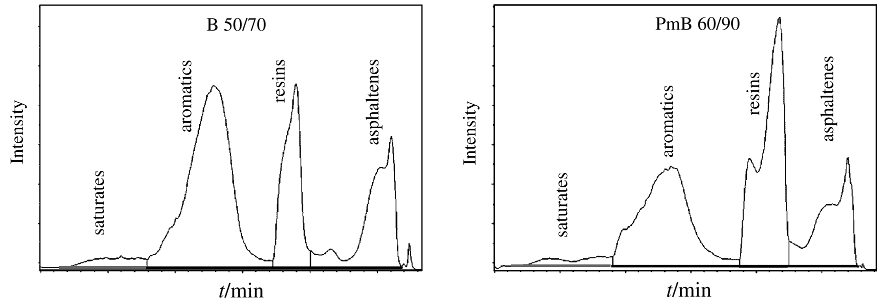


**Fig. 4.** Iatroscan chromatograms of B 50/70 and PmB 60/90 (normalized to 100)

**Table 3.** Generic fractions of Iatroscan analysis; *S* saturates, *A* aromatics, *R* resins, *As* asphaltenes

| Bitumen | *S* [%] | *A* [%] | *R* [%] | *As* [%] |
|---|---|---|---|---|
| B 50/70 | 3.6 | 52.4 | 22.7 | 21.3 |
| PmB 60/90 | 4.1 | 37.5 | 38.4 | 20.0 |

resins which amounts to 15%. This might be explained by the aromatic part (styrene) of the polymers associating with aromatics of bitumen, reflected by the increased resins peak during Iatroscan analysis.

### *Identification of Bitumen Microstructure*

During testing of bitumen with the environmental scanning electron microscope (ESEM), the exposure of the bitumen surface to the electron beam reveals a random string-like network structure also found in the work of *Rozeveld et al.* [5] and *Stangl et al.* [3]. It is hypothesized, that the electron beam volatilizes the low molecular weight fractions of the bitumen by localized heating, whereas the higher molecular weight fractions, *i.e.*, resins and asphaltenes, remain and become visible in the form of string-like structures as the surface oils have been removed (string-like structures embedded in a matrix substance). ESEM images of the considered types of bitumen after longer beam exposure are shown in Fig. 5. There are no distinct differences observed in microstructure between B 50/70 and PmB 60/90. This is explained by the use of B 50/70 as base bitumen for the production of the considered PmB 60/90, with the polymer not being present in the scan area.

In order to quantify the observed microstructure, the average diameter of the strings, $d$ [m], and the volume fraction of the strings in the bitumen microstructure, $f_s$ [−], were determined, following the procedure outlined in Ref. [3]. As listed in Table 4, the selected parameters for the description of the bitumen microstructure are quite similar for both types of bitumen.

### *Micromechanical Properties of Bitumen*

Figure 6 shows the histograms and the corresponding grid plots for the initial creep compliance $J_a$ of a parabolic dash-pot obtained from nanoindentation performed on a $10 \times 10$ grid on B 50/70 and PmB 60/90 tested at 9°C (see [12, 13] for the experimental procedure and analytical model). The grid plots confirm the microstructure observed by ESEM consisting of two distinct material phases with a typical dimension of approximately 10 $\mu$m. The histograms highlight the presence of these two phases, approximated by two Gaussian distributions. Each of them gives mean value and standard deviation of one of the two bitumen phases (string-like structure and matrix). Figure 6 also shows that the modified bitumen exhibits higher initial creep compliance values as the pure binder, which correlates with rheological properties obtained from the DSR experiments at 10°C shown in Figs. 1 and 2.

### *Thermoanalytical Behavior of Bitumen*

In contrast to materials showing a well-defined transfer from the glassy state to the amorphous state during temperature increase (glass transition), the molecular composition of bitumen results in glass transition regions distributed over a broad temperature range stemming from the formation and decomposition of "molecule clusters". In order to

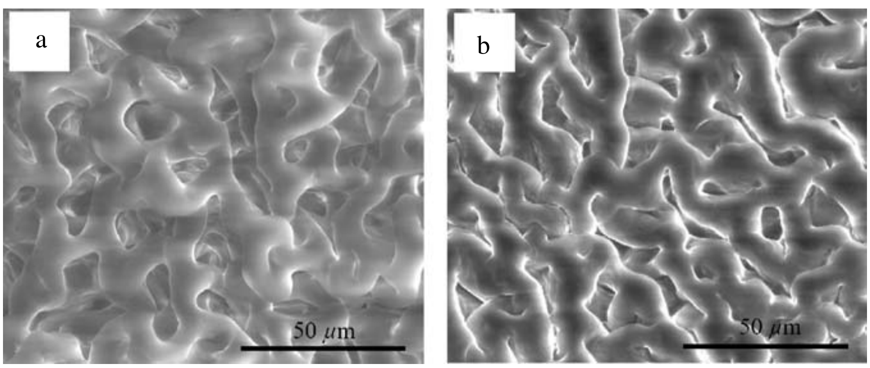


**Fig. 5.** ESEM images of (a) B 50/70 and (b) PmB 60/90 (pictures produced by "Research Institute for Electron Microscopy" at Graz University of Technology (Graz, Austria))

**Table 4.** Microstructural parameters from ESEM quantification; $d$ average diameter of the strings, $f_s$ volume fraction of strings in bitumen microstructure

| Bitumen | $d/\mu$m | $f_s$ |
|---|---|---|
| B 50/70 | 8.6 | 0.25 |
| PmB 60/90 | 10.0 | 0.33 |

determine the complex formation and decomposition of the bitumen microstructure, modulated differential scanning calorimetry (MDSC) was applied providing the reversing and non-reversing heat capacity (see Fig. 7 for B 50/70).

Similar to MDSC results reported in Refs. [6, 7], two (not very pronounced) glass transitions can be observed within $-50<T<0$°C and $40<T<80$°C. Based on the derivative of the reversing heat capacity, $dCp^{\mathrm{rev}}/dT$, depicted in Fig. 8, the respective values of the glass transition temperature ($T_g$), defined by the local maximum of $dCp^{\mathrm{rev}}/dT$, can be identified at $T\approx-20$°C and $T\approx+70$°C for both types of bitumen (see Table 5). The glass transitions are distributed over a temperature range of up to 50°C, which is explained by the complex chemical composition of bitumen, consisting of a wide range of different molecules as discussed previously in this chapter. The two glass transitions correspond to the two material phases, which have also been observed in ESEM and NI experiments.

Furthermore, the high temperature $T_g$ may be related to the larger molecules of bitumen, *i.e.* resins and asphaltenes, whereas the low temperature $T_g$ may be associated with low-molecular weight molecules, such as saturates and aromatics [7, 8]. Due to *SBS* modification an expansion of $\Delta T_g$ (from 87.8 to 96.3°C) is observed as highlighted in Fig. 8. This expansion indicates that the compatibility of the two material phases decreases with increasing polymer content. As additional information from Fig. 8, the area under the peak of each phase is an indicator for the amount of the corresponding phase involved in glass transition. Higher content of phase 2 (high temperature $T_g$) is observed for the PmB and *vice versa* for phase 1. This corresponds well with the Iatroscan results showing an increase of resins due to *SBS* modification.

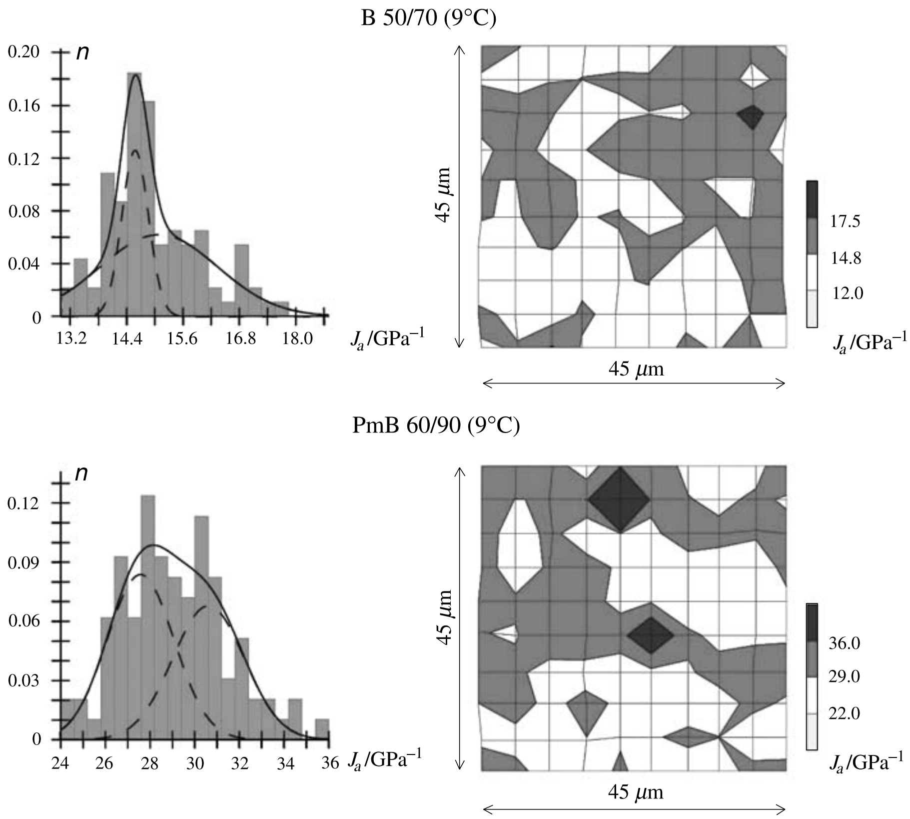


**Fig. 6.** Initial creep compliance $J_a$ for B 50/70 and PmB 60/90 obtained from nanoindentation performed at 9°C: histograms and corresponding grid plots

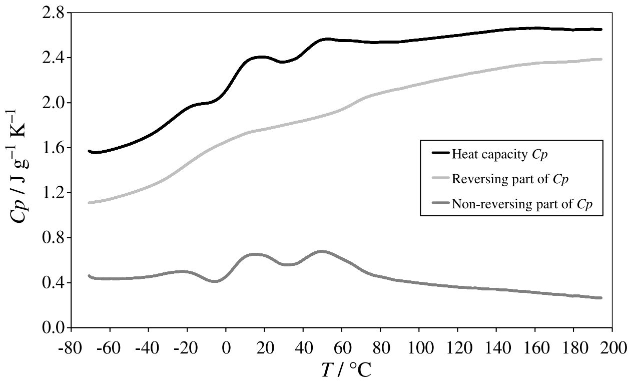


**Fig. 7.** Reversing and non-reversing heat capacity of B 50/70 from MDSC experiments

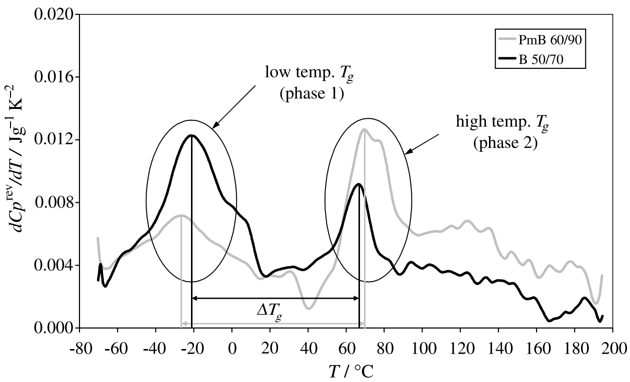


**Fig. 8.** Derivative of reversing heat capacity of B 50/70 and PmB 60/90

**Table 5.** Glass transition temperatures $T_g$ from MDSC experiments

| Bitumen | $T_{g,\text{low}}/°C$ | $T_{g,\text{high}}/°C$ |
|---|---|---|
| B 50/70 | −21.1 | 66.7 |
| PmB 60/90 | −26.5 | 69.8 |

## Experimental

*Types of Bitumen*

In order to cover the effect of *SBS* modification on the characteristics of bitumen, two types of bitumen, one plain bitumen and one polymer modified bitumen, provided by OMV Refining and Marketing GmbH (Vienna, Austria), are considered in the experimental program. Whereas a B 50/70 was used as plain bitumen, the polymer modified bitumen was obtained by the allowance of styrene-butadiene-styrene (*SBS*) to the aforementioned B 50/70, referred to as PmB 60/90 (the given numbers indicate the range of penetration according to Refs. [9, 10]). The modifier was a linear *SBS* block copolymer. As regards the production of the PmB 60/90 by the allowance of *SBS*, the polymer was soaked with oil at room temperature according to Ref. [11]. Thereafter, the soaked polymer is mixed with the B 50/70 at 190–200°C for 6 h.

*Methods*

Elemental analyses (C, H, N, O, S) were performed according to Ref. [12]. For the determination of the molecular weight distribution, gel permeation chromatography (GPC) was employed. Three fractionating columns (10000, 500 and 50 Å) were used with *THF* as running solvent at a constant speed of 1 cm$^3$/min. The GPC device was calibrated with polystyrene standards with mean values ranging from 162 to 1075000 g/mol. A refractive index detector was applied to detect the molecules passing through the columns which were recorded as a function of time. The weight average molecular weight ($M_w$) was obtained by multiplying the molecular weight values of each fraction by the respective mass fraction, as following:

$$M_w = \frac{\sum_i m_i M_i}{\sum_i m_i}, \tag{2}$$

where $m_i$ denotes the total weight of molecules with a molecular weight $M_i$.

In order to determine the generic composition, *i.e.*, the amount of the main constituents of the considered types of bitumen (saturates, aromatics, resins and asphaltenes), the Iatroscan method, combining thin layer chromatography with flame ionization detection (TLC/FID), was employed. The TLC/FID testing procedure was chosen similar to the one outlined in the work of *Friedbacher* [13]. First, 2% ($w/v$) solutions of bitumen were prepared in *THF*. Thereafter, 1 mm$^3$ of the sample solution was spotted onto so-called chromarods. Finally, the separation of bitumen into the four generic fractions due to differences in polarity was carried out by successive elution in $n$-heptane, toluene/$n$-heptane (80/20), and $CH_2Cl_2$/methanol (95/5). The amount of fractions was determined by means of an Iatroscan MK-5 TLC/FID analyzer from Iatron Laboratories Inc. The FID signals from each fraction are recorded as separate peaks in a chromatogram.

The ESEM experiments were conducted at the "Research Institute for Electron Microscopy" at Graz University of Technology (Graz, Austria). The pressure was set to 0.60 torr and an acceleration voltage of 20 keV was used. The samples were obtained by dropping bitumen on a sample holder. Images were taken not before 24 h after sampling.

For the identification of the mechanical properties at the micro-scale, nanoindentation (NI) was employed. During NI measurements, a tip with defined shape penetrates the specimen surface with the indentation load $P$ [N] and the penetration $h$ [m] recorded as a function of time. Each so-called "indent" during NI testing consists of a loading, holding, and unloading phase. The viscoelastic material properties of bitumen are identified from the holding phase using a single dash-pot model. The so-called grid indentation technique [14] is employed to extract information on the morphology of bitumen at the micro-scale. Hereby, several indents are performed on a specified grid (*e.g.*, 10 × 10 indents). With the characteristic dimension of the bitumen microstructure of 10 $\mu$m (diameter of strings) the distance between two adjacent grid points is set to 5 $\mu$m [15, 16].

Finally, modulated differential scanning calorimetry (MDSC) was used to determine phase-change temperatures and endo/exotherms associated with the destruction and formation of molecular arrangements. In contrast to standard DSC, the temperature increase in the temperature chambers of the MDSC device is performed in a modulated manner and allows distinguishing between the reversing and the non-reversing part of the total heat capacity. Only transitions which take place within a time scale smaller than the modulation period, *e.g.* glass transitions and melting, contribute to the reversing part, while processes with higher time scales, such as disorientation and re-organization of molecules, contribute to the non-reversing part according to Refs. [7, 17]. The results of MDSC measurements were obtained from a DSC Q1000 from TA Instruments. Bitumen samples were tested with an average heat rate of 3 K/min, a modulation amplitude of $\pm 0.5$ K/min, and an oscillation period of 60 s from $-80$ to 200°C.

## Acknowledgments

The authors thank *G. Lenk* and *A. Loibl* from OMV (Vienna, Austria) for providing results of gel permeation chromatography and elemental analyses. Furthermore, the authors are indebted to *Julian Wagner* from the "Research Institute for Electron Microscopy" at Graz University of Technology (Graz, Austria) for helpful support in the course of ESEM testing. Financial support by the Christian Doppler Gesellschaft (Vienna, Austria) is gratefully acknowledged.

## References

[1] Shell-Bitumen UK (1990) The Shell bitumen handbook, vol 1, Shell Bitumen UK, Chertsey
[2] Becker Y, Méndez MP, Rodríguez Y (2001) Vision Tecnologica **9**: 39
[3] Stangl K, Jäger A, Lackner R (2006) Int J Road Mater Pavement Design **7**: 111
[4] Steidl E (1992) Studien über den Nachweis von Styrol-Butadien-Copolymeren in Bitumen und deren Wechselwirungen mit Bitumen, Master's thesis, Vienna University of Technology, Vienna
[5] Rozeveld S, Shin E, Bhurke A, France L, Drzal L (1997) Microscopy Research Techn **38**: 529
[6] Masson JF, Polomark GM (2001) Thermochim Acta **374**: 105
[7] Jäger A (2004) Microstructural Identification of Bitumen by Means of Atomic Force Microscopy (AFM), Modulated Differential Scanning Calorimetry (MDSC), and Reflected Light Microscopy (RLM), Master's Thesis, Vienna University of Technology, Vienna
[8] Masson JF, Polomark GM, Collins P (2002) Energy Fuel **16**: 470
[9] ÖNORM EN 12591 (2005) Bitumen und bitumenhaltige Bindemittel – Anforderungen an Straßenbaubitumen, Österreichisches Normungsinstitut, 1020 Vienna
[10] ÖNORM B3613 (1999) Elastomermodifizierte Bitumen für den Straßenbau – Anforderungen, Österreichisches Normungsinstitut, 1020 Vienna
[11] Patent number AT397098 B, OMV Aktiengesellschaft, 1090 Vienna
[12] ASTM D5291 (2002) Standard test methods for instrumental determination of carbon, hydrogen and nitrogen in petroleum products and lubricants, ASTM International, West Conshohocken
[13] Friedbacher EC (1993) Qualitative und quantitative Gruppentrennung von Bitumen durch Dünnschichtchromatographie kombiniert mit Flammenionisationsdetektion, Dissertation, Vienna University of Technology, Vienna
[14] Ulm FJ, Delafargue A, Constandinides G (2005) In: Dormieux L, Ulm FJ (eds) Appl Micromech Porous Mat (CISM Courses and Lectures No. 480), Springer, Vienna
[15] Jäger A, Lackner R, Eberhardsteiner J (2006) Meccanica, in print
[16] Jäger A, Lackner R, Stangl K (2006) Int J Mat Res, in print
[17] Jiang Z, Imrie CT, Hutchinson JM (2002) Thermochim Acta **387**: 75–93